https://doi.org/10.1093/plphys/kiad425 PLANT PHYSIOLOGY 2023: 193: 2021–2036

Plant Physiology®

Research Article

Overlapping and specialized roles of tomato phytoene synthases in carotenoid and abscisic acid production

Miguel Ezquerro,[1,2] **Esteban Burbano-Erazo**[1] **and Manuel Rodriguez-Concepcion**[1,*]

1 Institute for Plant Molecular and Cell Biology (IBMCP), CSIC-Universitat Politècnica de València, Valencia 46022, Spain
2 Centre for Research in Agricultural Genomics (CRAG) CSIC-IRTA-UAB-UB, Barcelona 08193, Spain

*Author for correspondence: manuelrc@ibmcp.upv.es
The author responsible for distribution of materials integral to the findings presented in this article in accordance with the policy described in the Instructions for Authors (https://academic.oup.com/plphys/pages/General-Instructions) is: Manuel Rodriguez-Concepcion (manuelrc@ibmcp.upv.es).

Abstract

Carotenoids are plastidial isoprenoids required for photoprotection and phytohormone production in all plants. In tomato (*Solanum lycopersicum*), carotenoids also provide color to flowers and ripe fruit. Phytoene synthase (PSY) catalyzes the first and main flux-controlling step of the carotenoid pathway. Three genes encoding PSY isoforms are present in tomato, *PSY1* to *PSY3*. Mutants have shown that PSY1 is the isoform providing carotenoids for fruit pigmentation, but it is dispensable in photosynthetic tissues. No mutants are available for *PSY2* or *PSY3*, but their expression profiles suggest a main role for PSY2 in leaves and PSY3 in roots. To further investigate isoform specialization with genetic tools, we created gene-edited lines defective in PSY1 and PSY2 in the MicroTom background. The albino phenotype of lines lacking both PSY1 and PSY2 confirmed that PSY3 does not contribute to carotenoid biosynthesis in shoot tissues. Our work further showed that carotenoid production in tomato shoots relies on both PSY1 and PSY2 but with different contributions in different tissues. PSY2 is the main isoform for carotenoid biosynthesis in leaf chloroplasts, but PSY1 is also important in response to high light. PSY2 also contributes to carotenoid production in flower petals and, to a lesser extent, fruit chromoplasts. Most interestingly, our results demonstrate that fruit growth is controlled by abscisic acid (ABA) specifically produced in the pericarp from PSY1-derived carotenoid precursors, whereas PSY2 is the main isoform associated with ABA synthesis in seeds and salt-stressed roots.

Introduction

Carotenoids are a group of isoprenoid molecules synthetized by all photosynthetic organisms and some nonphotosynthetic bacteria and fungi (Rodriguez-Concepcion et al. 2018; Sun et al. 2018). Carotenoids are essential micronutrients in our diet as precursors of retinoids such as vitamin A. Their characteristic colors in the range of yellow to orange and red also make them economically relevant as natural pigments in the chemical, pharma, and agrofood industry. In plants, carotenoids are essential for photosynthesis (by contributing to the assembly and functioning of the photosynthetic apparatus) and for photoprotection (by dissipating the excess of light energy as heat and by scavenging free radicals). They also provide color to some nonphotosynthetic tissues such as flower petals and ripe fruit to attract animals for pollination and seed dispersal. Furthermore, carotenoids are precursors of the phytohormones abscisic acid (ABA) and strigolactones (SLs) as well as other biologically active signals involved in plastid-to-nucleus communication (e.g. beta-cyclocitral) and environmental interactions (e.g. apocarotenoids modulating root mycorrhization), among other processes (Moreno et al. 2021; Sun et al. 2018).

Received January 30, 2023. Accepted July 01, 2023. Advance access publication July 20, 2023

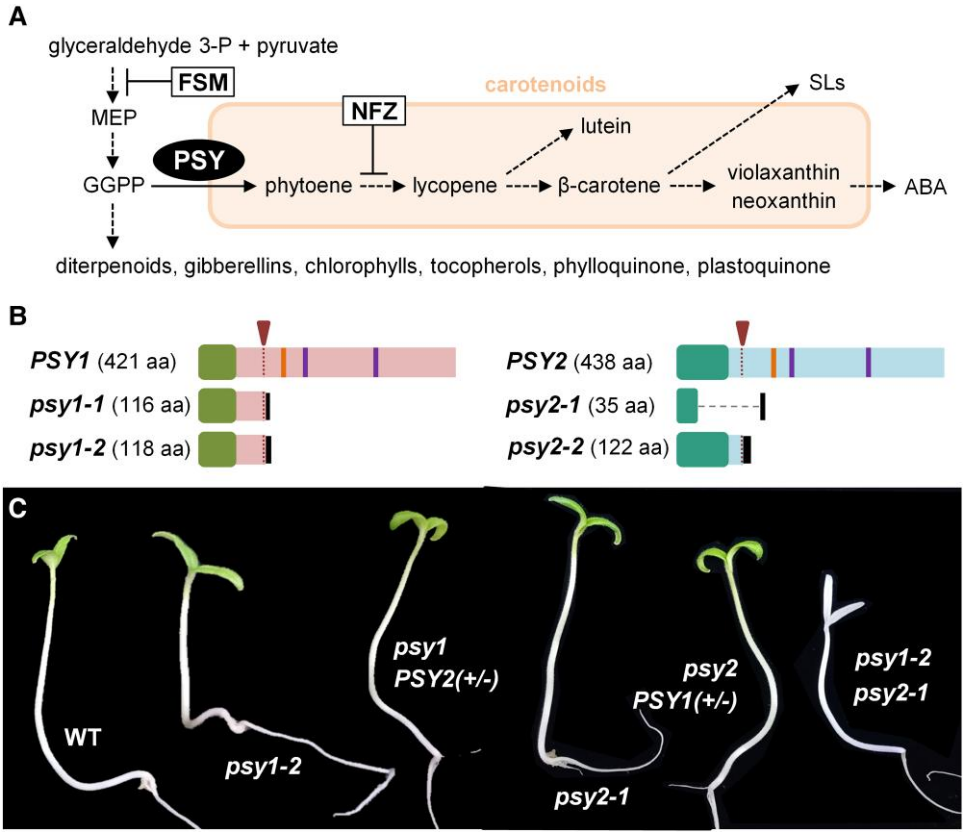

Figure 1. Carotenoid pathway and tomato mutants. **A)** Carotenoid biosynthesis pathway. Dashed arrows represent multiple steps. The reaction catalyzed by PSY is marked, and steps interrupted by inhibitors FSM and NFZ are indicated. MEP, methylerythritol 4-phosphate; GGPP, geranylgeranyl diphosphate; ABA, abscisic acid; SLs, strigolactones. **B)** Scheme representing the WT PSY1 and PSY2 proteins and the mutant versions generated in the corresponding CRISPR-Cas9–generated alleles (see Supplemental Figs. S1 to S3 for further details). The region targeted by the designed sgRNAs is indicated with an arrowhead and a dotted line. Vertical bars mark the position of conserved domains required for PSY activity (one hydrophobic flap and two Asp-rich domains). N-terminal boxes represent plastid transit peptides. C-terminal dark boxes represent the protein sequence resulting after a frameshift in the mutants. The large deletion generated in the *psy2-1* allele is shown with a dashed line. **C)** Representative 7-d-old seedlings of the indicated genotypes resulting from a cross of *psy1-2* and *psy2-1* mutants. Heterozygosis is indicated as "(+/-)" following the gene name, with the symbol "+" representing presence and "-" absence of the WT allele. Images were digitally extracted and they are shown to the same scale for comparison.

Carotenoids in plants are produced in plastids from geranylgeranyl diphosphate (GGPP) synthesized by the methylerythritol 4-phosphate (MEP) pathway (Fig. 1). MEP-derived GGPP is also used to produce diterpenoids, gibberellins, and photosynthesis-related isoprenoids such as plastoquinone, phylloquinone, tocopherols, and chlorophylls (Rodriguez-Concepcion et al. 2018). The first committed step of carotenoid biosynthesis is the condensation of 2 GGPP molecules to produce phytoene (Fig. 1A). This step is catalyzed by phytoene synthase (PSY), the main flux-controlling enzyme of the carotenoid pathway (Cao et al. 2019; Zhou et al. 2022). Several desaturation and isomerization steps convert uncolored phytoene into red lycopene. From lycopene, carotenoid synthesis branches out depending on the type of cyclization of the ends of the lycopene carbon chain. The production of 2 β rings at the 2 ends of the chain produces β-carotene (β,β branch) while the production of 1 β ring and 1 ε ring produces α-carotene (β,ε branch). Oxygenation of the rings of carotenes produces xanthophylls such as violaxanthin and neoxanthin (β, β branch) or lutein (β,ε branch) (Fig. 1A).

Tomato (*Solanum lycopersicum*) is a very well-suited model system to study carotenoid biosynthesis. Like all plants, tomato produces carotenoids for photosynthesis and photoprotection in chloroplasts and uses them as precursors to produce ABA and SLs in photosynthetic and nonphotosynthetic tissues. But unlike Arabidopsis (*Arabidopsis thaliana*) and other plant models, tomato accumulates high levels of carotenoids in specialized plastids named chromoplasts, which are present in flower petals and ripe fruit. Also different from Arabidopsis, which only has a single PSY (At5g17230), the tomato genome harbors 3 PSY-encoding genes: *PSY1* (Solyc03g031860), *PSY2* (Solyc02g081330), and *PSY3* (Solyc01g005940) (Giorio et al. 2008; Stauder et al. 2018). While PSY1 and PSY2 are similar proteins that share conserved sequences and have a common origin (Cao et al. 2019; Giorio et al. 2008), tomato PSY3 belongs to a different clade restricted to dicots (Stauder et al. 2018). Dicot-type PSY3 sequences show an ancient origin and a strong association with root mycorrhization and SL production, whereas the PSY3 sequences found in monocots such as rice

(*Oryza sativa*) and maize (*Zea mays*) are phylogenetically related to PSY1 and PSY2 isoforms and they are involved in ABA biosynthesis in roots exposed to drought or salt stress (Li et al. 2008; Welsch et al. 2008; Stauder et al. 2018). Tomato lines defective in PSY1 have been reported as *yellow-flesh* (*r*) mutants (Fray and Grierson 1993; Kachanovsky et al. 2012; Kang et al. 2014; Karniel et al. 2022), silenced lines (Bird et al. 1991; Bramley et al. 1992; Fantini et al. 2013; Fraser et al. 1999) and CRISPR-Cas9–edited lines (D'Ambrosio et al. 2018), but lines impaired in PSY2 or PSY3 have not been described yet. Based mostly on sequence homology and gene expression data, it was proposed that tomato PSY3 function might be restricted to the production of SLs and other apocarotenoids in roots whereas PSY1 and PSY2 appear to differentially support carotenogenesis in shoot tissues: PSY1 for pigmentation in chromoplasts and PSY2 for photosynthesis in chloroplasts (Fraser et al. 1999; Giorio et al. 2008; Hirschberg 2001; Stauder et al. 2018; Ezquerro et al. 2023). However, other sources of evidence suggest that isoform specialization is not complete. For example, the low but statistically significant up-regulation of *PSY1* during seedling deetiolation (when carotenoids are essential for the proper assembly of the photosynthetic apparatus and for photoprotection) and the high levels of *PSY2* transcripts in flower petals (where accumulation of xanthophylls is responsible for their characteristic yellow color) allow to hypothesize that both isoforms might participate in carotenoid biosynthesis in chloroplasts and chromoplasts (Barja et al. 2021; Giorio et al. 2008). To genetically test this hypothesis, we created tomato edited lines defective in PSY1 and PSY2 in the same background (MicroTom, a widely used accession in molecular biology labs all over the world) and compared their physiological and metabolic phenotypes. The albino phenotype of lines defective in both PSY1 and PSY2 confirmed that PSY3 does not contribute to carotenoid biosynthesis in shoot tissues. Our work further confirmed that PSY2 is the main isoform supporting chloroplast carotenoid biosynthesis but uncovered a role for PSY1 under conditions requiring an extra supply of carotenoids such as high light (HL) exposure. PSY1 was confirmed to be the main isoform in charge of phytoene production for carotenoid pigments in the chromoplasts of flower petals and fruit pericarp. Most interestingly, lower carotenoid levels resulted in a preferential reduction of ABA levels in the fruit pericarp but not in the leaves, roots, or seeds of the *psy1* mutant, whereas loss of PSY2 caused a major reduction of ABA in seeds and salt-treated roots. The differential ABA decrease in different fruit tissues of *psy1* and *psy2* mutants allowed us to unveil a specific contribution of pericarp ABA to fruit growth and seed ABA to seed germination.

Results

Loss of both PSY1 and PSY2 causes an albino lethal phenotype

To generate plants defective in PSY1 or/and PSY2 in the MicroTom background, we designed 1 single guide RNA (sgRNA) annealing on the start of the first translated exon for each gene using the online tool CRISPR-P 2.0 (Liu et al. 2017). Two independent alleles with premature translation stop codons were selected for each gene and named *psy1-1*, *psy1-2*, *psy2-1*, and *psy2-2* (Fig. 1B; Supplemental Figs. S1 to S3). For subsequent experiments, we selected homozygous lines of each allele without the Cas9-encoding transgene. In the case of *psy1-1* and *psy1-2* alleles, we observed paler yellow flowers and pale orange fruits (Supplemental Fig. S4), which are previously described phenotypes of PSY1-defective *r* tomato lines, hence confirming that both were loss of function mutants. No distinctive phenotype was observed in the case of *psy2-1* and *psy2-2* lines. Analysis of transcript levels in fruits by reverse transcription quantitative PCR (RT-qPCR) showed that loss of one of the isoforms did not influence the expression of the remaining genes (Supplemental Fig. S4).

To assess the impact of simultaneous disruption of PSY1 and PSY2, we crossed lines defective in PSY1 (*psy1-2*, as female) and PSY2 (*psy2-1*, as male). Double heterozygous F_1 plants with normal yellow flowers and red fruits were obtained and allowed to self-pollinate. Among the segregating F_2 population, we found several albino seedlings with a Mendelian proportion (1/16) consistent with this phenotype being the result of the loss of both PSY1 and PSY2 in double mutant individuals (Fig. 1C). The rest of the seedlings of the F_2 population displayed a normal green phenotype indistinguishable from the MicroTom wild-type (WT). PCR-based genotyping allowed to identify WT alleles (represented as "+") and mutant alleles (represented as "-") for each of the 2 genes in the segregating population (Supplemental Fig. S5). This analysis confirmed that green seedlings harbored at least 1 WT copy of either *PSY1* or *PSY2* whereas all albino seedlings were double homozygous mutants. The results indicate that PSY1 and PSY2 (but not PSY3) are essential for the production of carotenoids supporting seedling establishment and photosynthetic shoot development. Consistently, *PSY3* transcripts are hardly detectable in shoot tissues whereas *PSY1* and *PSY2* transcripts are abundant in all tissues of the tomato plant (Barja et al. 2021; Giorio et al. 2008; Stauder et al. 2018) (Supplemental Fig. S6).

PSY2 but also PSY1 contribute to produce carotenoids for photoprotection in leaves

To test whether carotenoid levels were reduced in leaves of single *psy1* and *psy2* mutant lines, we collected young emerging leaves from plants grown for 18 d under long-day conditions in the greenhouse and used them for HPLC analysis of carotenoids and chlorophylls (Fig. 2). Despite WT and mutant plants were phenotypically identical (Fig. 2A), a slight reduction in carotenoid levels was detected in mutant leaves compared to WT controls (Fig. 2B). Chlorophylls were not as reduced as carotenoids (Fig. 2B). These results suggest that both PSY1 and PSY2 can produce carotenoids in chloroplasts under normal growth conditions. Most interestingly,

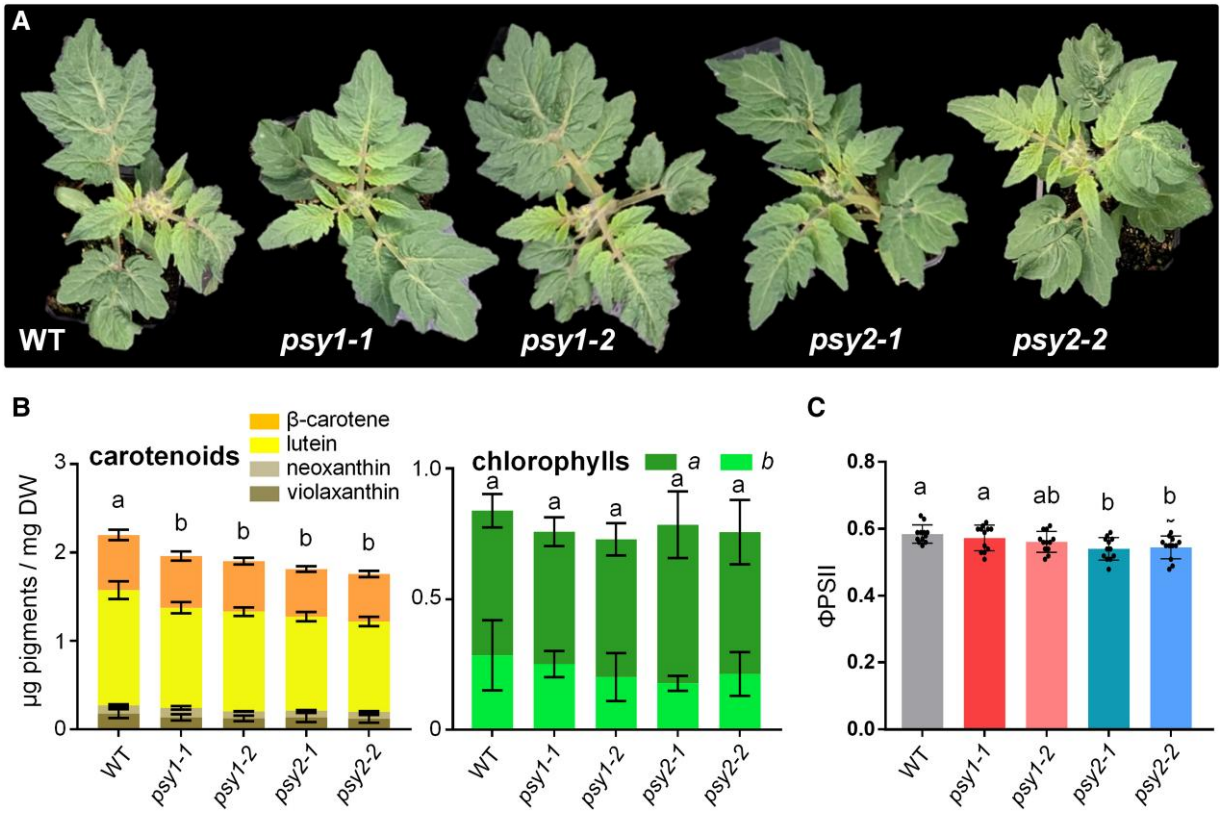

Figure 2. Tomato mutants defective in PSY1 or PSY2 show lower carotenoid levels under normal growth conditions. **A)** Representative images of 4-wk-old plants of the indicated lines. Images were digitally extracted and they are shown to the same scale for comparison. **B)** Total levels of carotenoids and chlorophylls in young leaves of WT and mutant plants like those shown in **A)**. Mean and SD of $n \geq 3$ independent biological replicates are shown. DW, dried weight. **C)** ΦPSII in young leaves like those used in **B)**. Individual values (black dots) as well as mean and SD are shown, and they correspond to 4 different leaf areas from 3 different plants. In **B)** and **C)**, letters represent statistically significant differences ($P < 0.05$) among means according to post hoc Tukey's tests run when 1-way ANOVA detected different means.

photosynthetic performance was only significantly reduced in *psy2* mutant alleles, as estimated from effective quantum yield of photosystem II (ΦPSII) measurements (Fig. 2C).

The main role of carotenoids in photosynthetic organs such as leaves is photoprotection against photooxidative damage associated with intense light. In particular, carotenoids can dissipate the excess light energy as heat through a process known as nonphotochemical quenching (NPQ). Consistent with this essential function of leaf carotenoids, when 10-d-old tomato seedlings grown under normal light (NL) conditions (50 μmol photons m^{-2} s^{-1}) were transferred to HL conditions (300 μmol photons m^{-2} s^{-1}) for 5 d, expression of genes encoding PSY1 and PSY2 and concomitant production of carotenoids were upregulated compared to control plants transferred for the same time to NL (Fig. 3). *PSY3* transcripts were undetectable in leaves from NL or HL samples (Fig. 3A), whereas chlorophylls remained virtually unchanged (Fig. 3B). The increase in carotenoid levels associated with HL exposure of WT plants was significantly repressed in *psy2* mutants and, to a lower extent, in *psy1* mutants (Fig. 3C). The potential photosynthetic capacity estimated from the measurement of F_v/F_m was reduced in leaves of *psy2* seedlings grown under normal conditions (Fig. 3D), similar to that observed for ΦPSII in young leaves (Fig. 2C). When exposed to HL, F_v/F_m decreased in both PSY-defective mutants, but the drop was stronger in *psy2* seedlings (Fig. 3D). NPQ was also reduced in HL-exposed *psy1* and *psy2* mutants compared to WT controls, with *psy2* seedlings showing lower values than *psy1* alleles (Fig. 3E). These results suggest a primary role for PSY2 and a secondary role for PSY1 in supplying phytoene when enhanced carotenoid synthesis is needed for photoprotection. A reduction of PSY1 activity in homozygous *psy2-1* mutants with the *psy1-2* mutation in heterozygosis, herein referred to as *psy2 PSY1*(+/-), did not significantly alter carotenoid levels, F_v/F_m, or NPQ compared to *psy2-1* seedlings (Fig. 3). Similarly, *psy1 PSY2*(+/-) seedlings were indistinguishable from the *psy1-2* parents (Fig. 3). The absence of a dose effect suggests that PSY1 and PSY2 might not be fully interchangeable in leaves requiring extra carotenoid synthesis such as those exposed to HL.

PSY1 is the main isoform producing carotenoids for flower and fruit pigmentation

Besides their essential role in chloroplasts, carotenoids accumulate in specialized plastids named chromoplasts that provide distinctive yellow, orange, and red colors to nonphotosynthetic

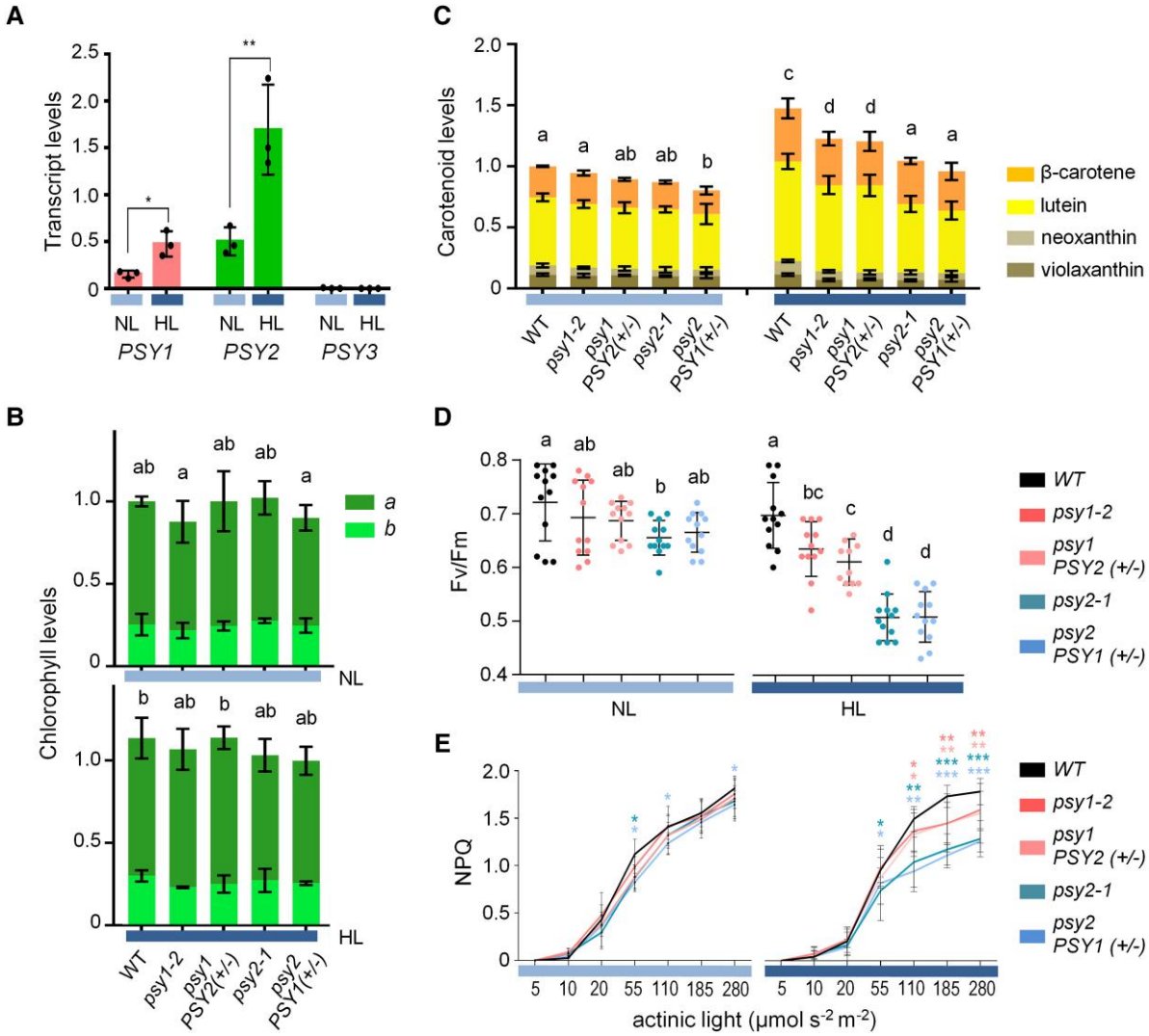

Figure 3. PSY2 is the main isoform required for photoprotection. Tomato WT and mutant seedlings germinated and grown for 10 d under normal light (NL) conditions were left for 5 more days under the same light conditions (NL) or transferred to higher light (HL) for the same time. **A)** RT-qPCR analysis of *PSY1*, *PSY2*, and *PSY3* transcript levels in WT seedlings at the end of the experiment normalized using *ACT4*. Data correspond to mean and SD of $n = 3$ independent biological replicates. **B)** Total chlorophyll levels in WT and mutant seedlings exposed to either NL or HL. **C)** Carotenoid levels in the samples described in **B)**. **D)** F_v/F_m values in WT and mutant lines during the indicated treatments. **E)** NPQ values at the indicated times of exposure to either NL or HL upon increasing actinic light. In **B)** and **C)**, mean and SD of $n = 3$ independent biological replicates are shown relative to those in WT NL controls. In **D)** and **E)**, values represent the mean and SD of 4 different leaf areas from 3 different seedlings. In **B** to **D)**, letters represent statistically significant differences ($P < 0.05$) among means according to post hoc Tukey's tests run when 1-way ANOVA detected different means. In **A)** and **E)**, asterisks indicate statistically significant differences among means relative to NL **A)** or WT **E)** samples (*t* test: $^*P < 0.05$; $^{**}P < 0.01$, $^{***}P < 0.001$).

tissues such as flower petals and ripe fruit. In tomato, carotenoids (mainly conjugated xanthophylls) are responsible for the yellow color of flower petals (Fig. 4) (Ariizumi et al. 2014). As previously reported for PSY1-defective lines (Bird et al. 1991; Bramley et al. 1992; Fraser et al. 1999), *psy1-1* and *psy1-2* alleles showed flowers of a paler yellow color than the WT (Fig. 4A; Supplemental Fig. S4). HPLC analysis of free and conjugated xanthophyll content showed a reduction of about 50% in PSY1-defective compared to WT corollas (Fig. 4B). While the absence of *PSY3* transcripts in flowers (Supplemental Fig. S6) suggests that PSY2 feeds the production of the carotenoids detected in PSY1-defective fruit, a reduction of PSY2 activity in *psy1 PSY2*(+/-) lines resulted in only a modest reduction in carotenoid levels compared to *psy1* flowers (Fig. 4B). Both *psy2-1* and *psy2-2* mutant alleles showed normal-looking flowers (Fig. 4A) with a virtually WT carotenoid profile (Fig. 4B), but carotenoid levels were slightly reduced in flowers of *psy2 PSY1*(+/-) plants (Fig. 4B). We therefore conclude that an excess of PSY1 activity ensures enough carotenoid production in tomato flower corollas.

The most characteristic phenotype of PSY1-defective tomato lines is the yellow color of the ripe fruit (Bird et al. 1991; D'Ambrosio et al. 2018; Fraser et al. 1999; Fray and Grierson 1993; Gupta et al. 2022; Kachanovsky et al. 2012;

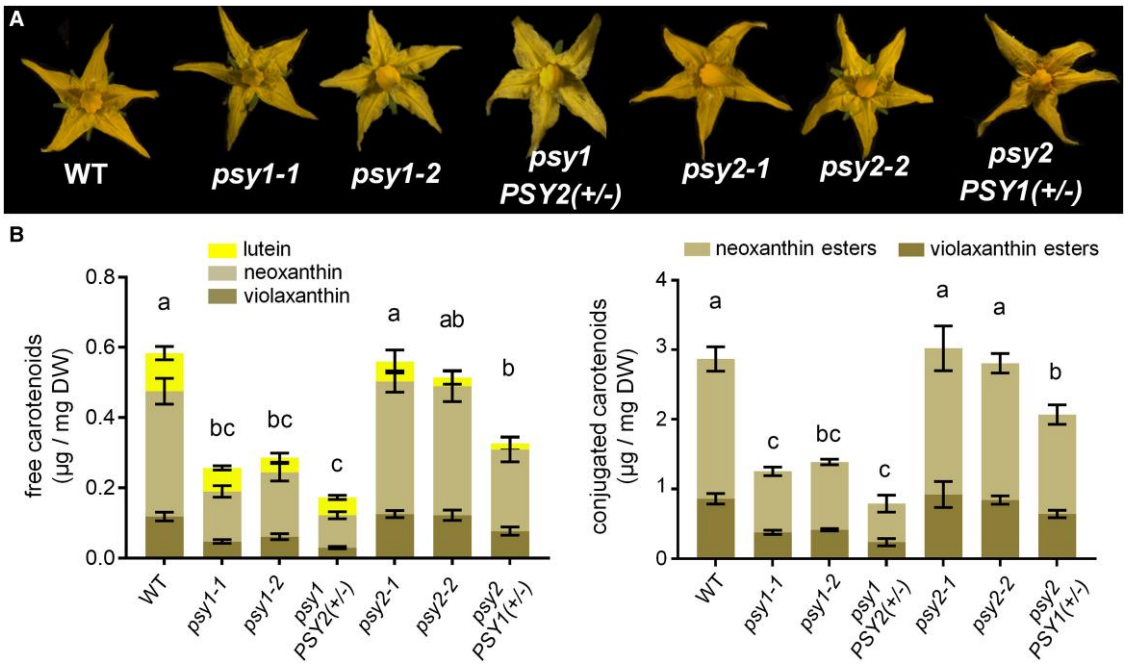

Figure 4. PSY1 is the main isoform contributing to carotenoid biosynthesis in petal chromoplasts. **A)** Representative images of anthesis (fully open) flowers of the indicated lines. Images were digitally extracted and they are shown to the same scale for comparison. **B)** Total levels of free and conjugated carotenoids in petals. Mean and SD of $n = 3$ independent biological replicates are shown. Letters represent statistically significant differences ($P < 0.05$) among means according to 1-way ANOVA followed by post hoc Tukey's tests.

Kang et al. 2014; Karniel et al. 2022). Tomato fruit ripening is a carotenoid-demanding process as great amounts of lycopene and, to a lower extent, β-carotene are produced to provide the characteristic red and orange color to the ripe fruit flesh: the pericarp (Fig. 5). Besides carotenoid synthesis, ripening also involves degradation of chlorophylls after the fruit reaches its final size at the mature green (MG) stage, which changes the fruit color from the breaker (B) stage (Fig. 5A). Previous reports have shown that loss of PSY1 activity does not impact carotenoid levels at the MG stage but it results in a drastic reduction in pericarp carotenoid levels in ripe fruit, which show a yellowish color due to flavonoid compounds such as naringenin chalcone (D'Ambrosio et al. 2018; Fraser et al. 1999; Fray and Grierson 1993; Kachanovsky et al. 2012; Kang et al. 2014). Consistently, our edited lines lacking PSY1 showed WT carotenoid and chlorophyll levels in the pericarp of MG fruit (Fig. 5B). Also as expected, analysis of pericarp carotenoid contents at 6 d after the B stage (B + 6) showed extremely low (but still detectable) levels of carotenoids (lutein and β-carotene) in PSY1-defective fruit (Fig. 5C). To investigate the contribution of PSY2 to the residual carotenoid contents of B + 6 (i.e. ripe) fruit with a complete loss of PSY1, we compared the carotenoid profile of *psy1-2* and *psy1 PSY2*(+/-) fruit. A reduction in total carotenoids was observed in *psy1 PSY2*(+/-) relative to *psy1-2* fruit (Fig. 5C) but it was only statistically significant for β-carotene. In agreement with the conclusion that PSY1 is by far the main contributor to carotenoid production in the pericarp of ripe fruit, complete loss of PSY2 in single *psy2-1* mutant fruit had no impact in carotenoid levels compared to WT fruit whereas a statistically significant reduction of pigment contents was found when PSY1 activity was genetically reduced in *psy2 PSY1*(+/-) fruit (Fig. 5C).

After the B stage, our *psy1-2* and *psy1 PSY2*(+/-) fruits acquired a distinctive yellowish color but PSY2-defective *psy2-1* and *psy2 PSY1*(+/-) fruits were undistinguishable from WT fruits (Fig. 5A). Color analysis using Tomato Analyzer showed that color changes in *psy1* fruits occurred at a lower rate compared to *psy2* mutant and WT controls (Fig. 6A). To test whether mutant fruit showed other ripening-associated phenotypes besides color change, the expression of ripening marker genes such as *E8* (Solyc09g089580) and *ACS2* (Solyc01g095080) was quantified by RT-qPCR (Barja et al. 2021). As shown in Fig. 6B, the expression profile of these genes was very similar in WT and *psy2-1* fruit during ripening. By contrast, the peak of *E8* and *ACS2* expression observed at the B stage was significantly reduced in *psy1-2* fruit (Fig. 6B). Both *E8* and *ACS2* are associated to the production of ethylene, a hormone that regulates many aspects of the ripening process in climacteric fruits such as tomatoes (Diretto et al. 2020; McQuinn et al. 2020; Zhang et al. 2009). However, levels of ethylene emitted by harvested fruits were similar in all lines at the B and B + 3 stages (Fig. 6C). Similarly, fruit hardness of *psy1* fruit at B, B + 3, and B + 6 was not changed compared to *psy2* and WT controls (Fig. 6D). All these data together support the

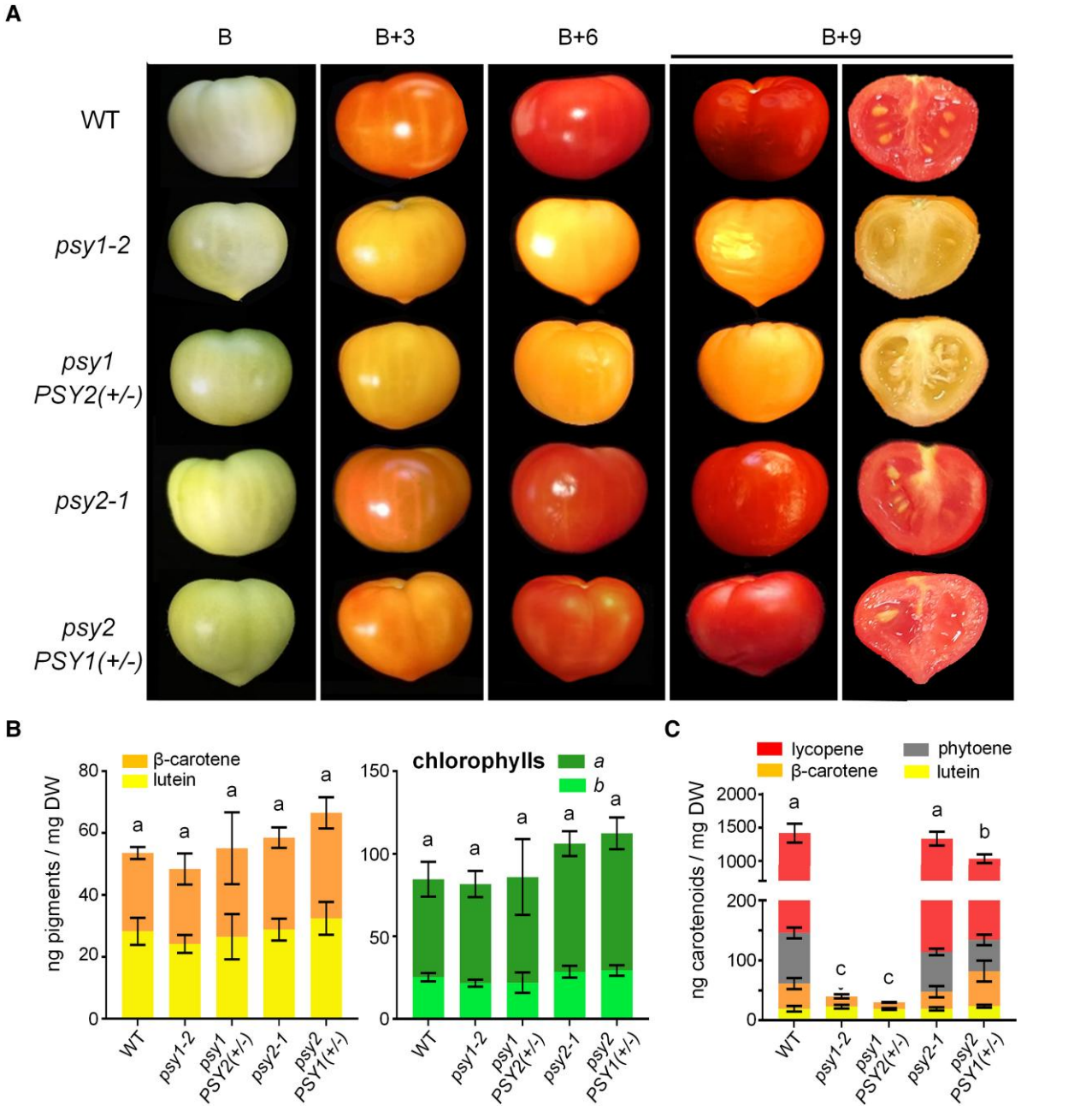

Figure 5. PSY1 is the main isoform contributing to carotenoid biosynthesis in fruit pericarp chromoplasts. **A)** Representative images of WT and mutant fruit collected at the B stage and left to ripen off-vine in a controlled environment chamber for the indicated times (in days). Images were digitally extracted and they are shown to the same scale for comparison. **B)** Total carotenoid and chlorophyll levels in WT and mutants in the pericarp of fruit collected from the plants at the MG stage. **C)** Total carotenoid levels in WT and mutants in the pericarp of fruit collected from the plants at the B + 6 stage. In all the plots, mean and SD of $n = 3$ independent biological replicates are shown. Letters represent statistically significant differences ($P < 0.05$) among means according to post hoc Tukey's tests run when 1-way ANOVA detected different means.

conclusion that the fruit ripening process is not substantially altered in PSY1-defective fruit.

PSY1 and PSY2 differentially contribute to ABA synthesis in tomato fruit, seeds, and roots

ABA is a carotenoid-derived phytohormone (Fig. 1A) which, besides regulating plant adaptation to abiotic stress conditions and promoting seed dormancy, appears to regulate fruit growth and development in tomato (Leng et al. 2014; Nambara and Marion-Poll 2005; Zhang et al. 2009). Indeed, reduced hormone levels in mutants defective in ABA biosynthetic genes such as *notabilis* (*NOT*/*NCED*), *sitiens* (*SIT*/*AAO3*), and *flacca* (*FLC*/*ABA3*) are associated to slower ripening, reduced fruit size, and accelerated seed germination

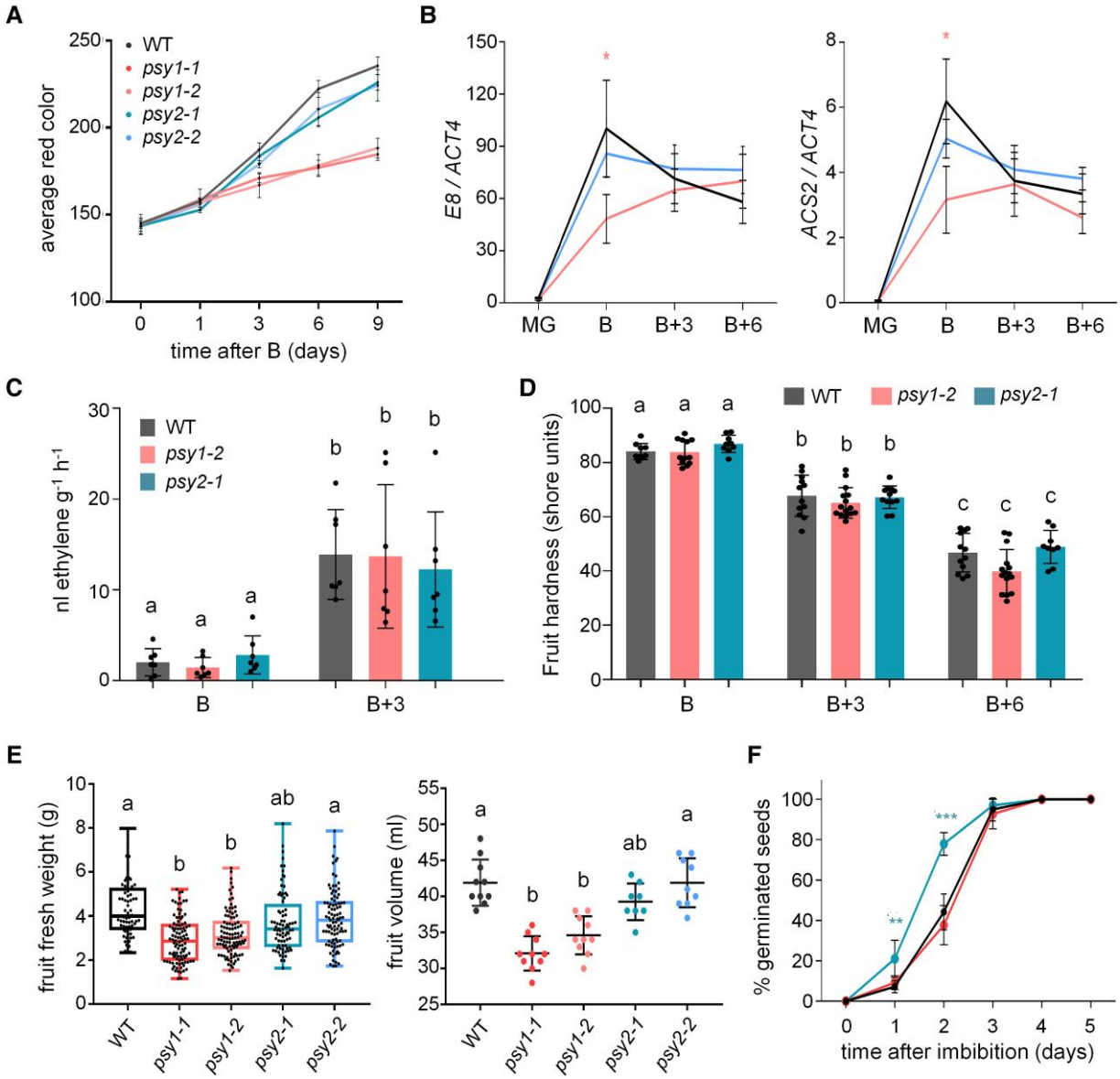

Figure 6. Fruit development and seed germination are differentially impacted in mutants defective in PSY1 or PSY2. **A)** Average red color quantification (arbitrary units) of fruit collected at the B stage and left to ripen in chambers for the indicated times. **B)** RT-qPCR analysis of *E8* and *ACS2* transcript levels in fruits collected from the plant at the indicated stage. In **A)** and **B)**, values represent the mean and SD of $n = 3$ different fruits for each time point. **C)** Ethylene production of whole fruits collected at the B stage and left to ripen off-vine. Each dot represents an individual fruit. **D)** Hardness of WT and mutant fruit at the indicated ripening stage represented as shore (durometer) units as a measure of the resistance to indentation. Each dot represents the mean value of 3 measurements in an individual fruit. In **C)** and **D)**, mean and SD of the indicated data points are shown. **E)** Weight and volume of fully ripe fruits of the indicated genotypes. In the boxplot, the lower and upper boundaries of the boxes indicate the 25th and 75th percentiles, respectively; the line inside the boxes represents the median; dots mark individual data values; and whiskers above and below the boxes indicate the maximum and minimum values. In the dot plots, central line represents the mean and whiskers represent SD. **F)** Germination kinetics of WT and mutant seeds after imbibition. Error bars indicate SD of $n = 6$ biological replicates with 25 seeds each. In **B)** and **F)**, asterisks indicate statistically significant differences among means relative to WT samples (*t* test: $^*P < 0.05$; $^{**}P < 0.01$, $^{***}P < 0.001$). In **C** to **E)**, different letters represent statistically significant differences (1-way ANOVA followed by Tukey's multiple comparisons test, $P < 0.05$).

(De Castro and Hilhorst 2006; Galpaz et al. 2008; Groot and Karssen 1992; McQuinn et al. 2020; Nitsch et al. 2012). ABA levels in pericarp and seeds peak around the B stage, preceding the burst of ethylene biosynthesis (Berry and Bewley 1992; De Castro and Hilhorst 2006; Diretto et al. 2020; Zhang et al. 2009). Quantification of ABA in pericarp and seed samples from WT and mutant fruit at the B stage showed decreased levels of the hormone in the pericarp of *psy1-2* fruit and the seeds of *psy2-1* samples (Fig. 7). Consistent with the decrease in pericarp ABA levels, fruits lacking PSY1 showed lower fruit weight and volume compared to WT and PSY2-defective fruits (Fig. 6E). We also

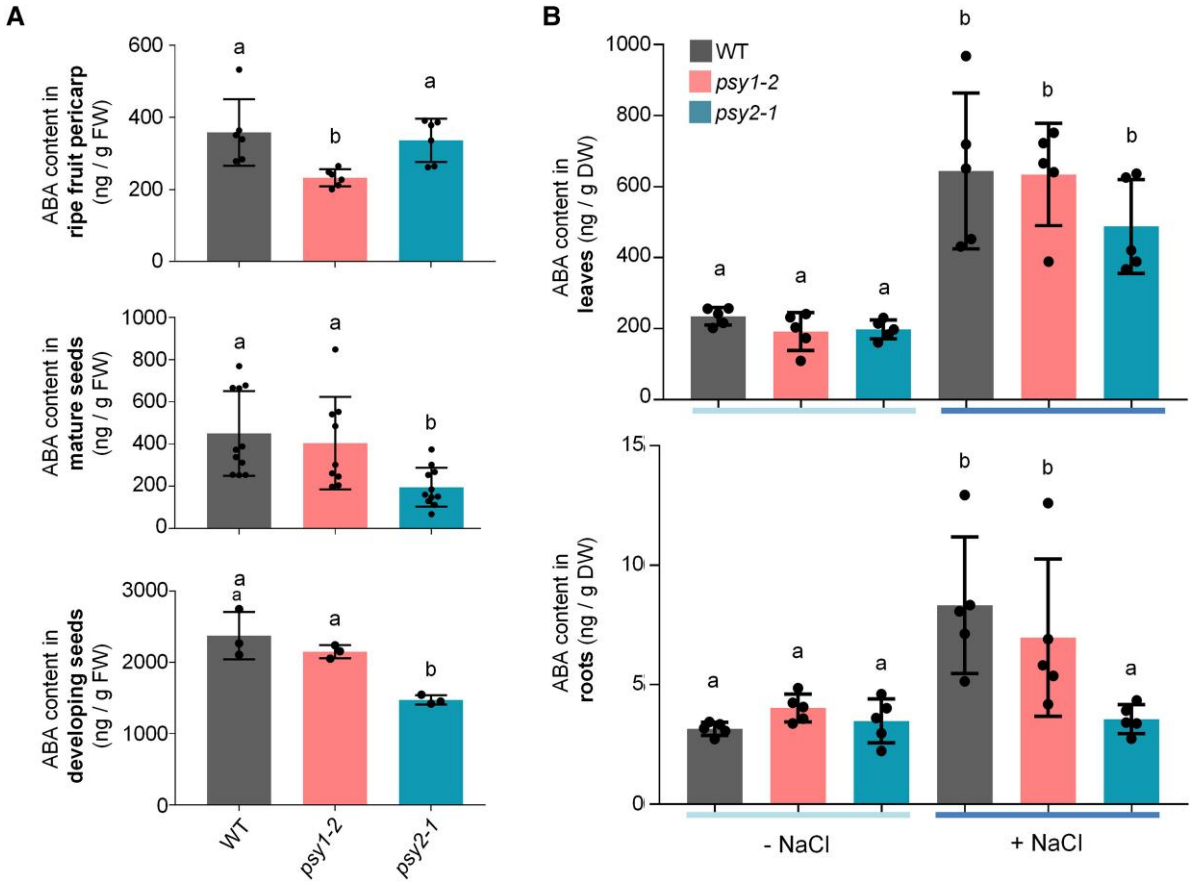

Figure 7. PSY1 and PSY2 differentially contribute to ABA production in specific tissues. **A)** ABA levels in tomato fruit pericarp and seeds. Pericarp and mature seed samples were collected from ripe (B + 6) fruit, whereas developing seeds were collected from immature fruits. **B)** ABA levels in leaves and roots of hydroponically grown tomato seedlings incubated with salt (+NaCl) or a mock solution (-NaCl) for 24 h. Individual values (black dots) as well as mean and SD are shown. Different letters represent statistically significant differences among means (1-way ANOVA followed by Tukey's multiple comparisons test, $P < 0.05$).

analyzed the germination (root emergence) of WT and mutant seeds freshly collected from ripe fruits. Accordingly to the reduced levels of ABA in the seeds of PSY2-defective mutants (Fig. 7A), *psy2-1* seeds showed an accelerated germination compared to WT and *psy1-2* seeds (Fig. 6F).

The described data suggest that PSY1 might be most important for ABA production in the pericarp and PSY2 in seeds. This conclusion is only partially consistent with transcript abundance profiles during fruit pericarp and seed development (Supplemental Figs. S6 to S8). In the pericarp, *PSY1* is expressed at higher levels than *PSY2* from early stages of fruit development, and the differences become much more dramatic after the MG stage (Supplemental Figs. S6 and S7). By contrast, both genes are expressed at similar levels in developing seeds (Supplemental Figs. S6 and S8) and yet ABA contents are reduced in the *psy2-1* mutant but not in the *psy1-1* line when compared to the WT (Fig. 7). As fruits ripen, *PSY1* expression increases and *PSY2* expression decreases in mature seeds (Supplemental Figs. S6 and S8), which similar to developing seeds only show reduced ABA levels when PSY2 activity is removed (Fig. 7). To provide complementary evidence on the role of PSY2 isoforms in the production of seed ABA, we compared the dormancy phenotype of freshly harvested seeds from *psy2* and carotenoid-devoid fruit (Fig. 8). To mimic complete loss of PSY activity and carotenoid production, we used the MEP pathway inhibitor fosmidomycin (FSM) and the phytoene desaturase inhibitor norflurazon (NFZ) (Fig. 1A). WT, *psy1-2*, and *psy2-1* fruits were collected from the plant at the MG stage and injected with one of the inhibitors or a mock solution (water). After 12 d, WT and *psy2-1* fruits treated with either FSM or NFZ showed a yellow color identical to that of *psy1-2* fruit treated with mock or inhibitor solutions (Fig. 8A), confirming that both FSM and NFZ successfully prevented downstream carotenoid production in fruit tissues. At this point, seeds were collected from the detached fruits, left to dry overnight, and immediately used for germination assays (Fig. 8B). In the case of WT and *psy1-2* seeds, germination was accelerated by the treatment with either FSM or NFZ, in agreement with the expected inhibitor-mediated blockage of carotenoid and hence downstream ABA

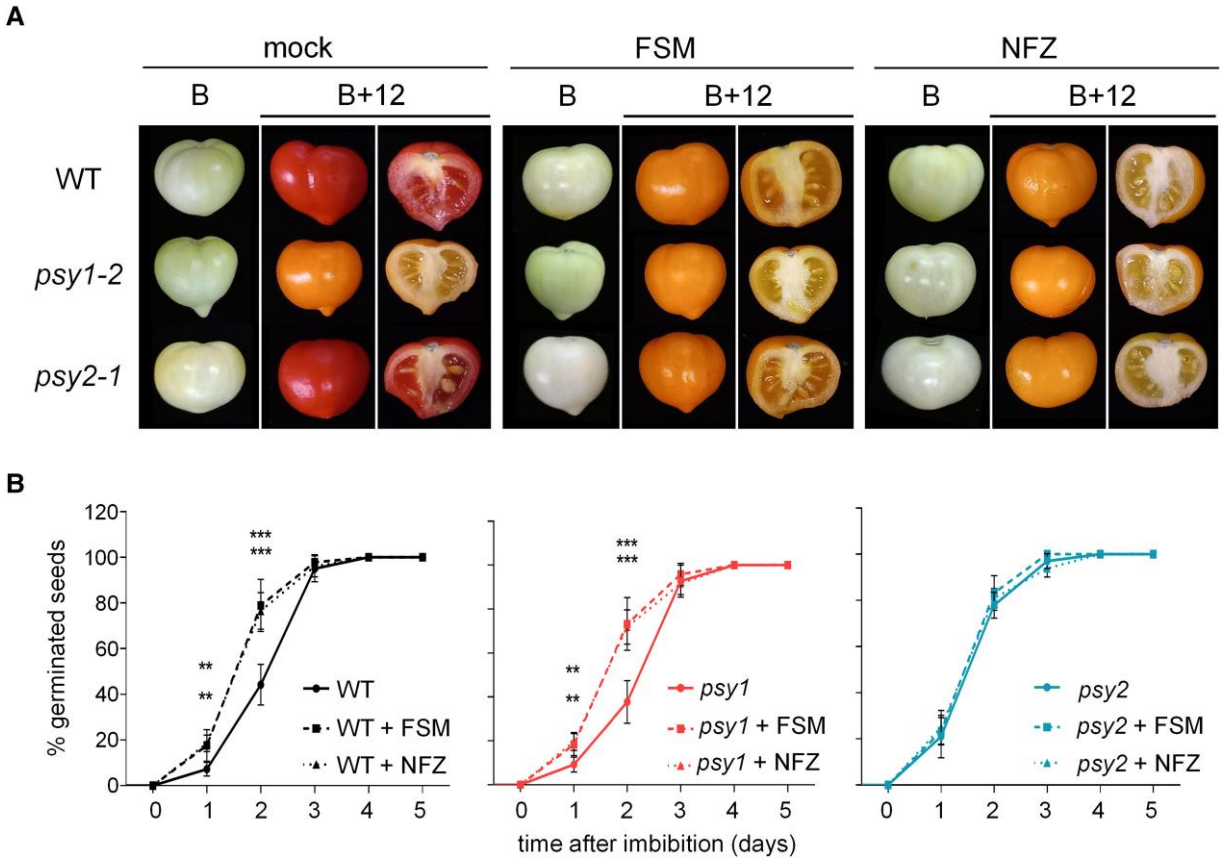

Figure 8. Germination of tomato seeds is regulated by ABA produced in mature seeds from PSY2-derived carotenoids. **A)** Representative images of WT and mutant fruits treated with FSM, NFZ, or a mock solution at the MG stage and then allowed to ripen off-vine. Images were digitally extracted and they are shown to the same scale for comparison. **B)** Kinetics of germination of fresh seeds collected from fruits as those shown in **A)** at the B + 12 stage. Error bars indicate SD of $n = 6$ biological replicates with 25 seeds each. Asterisks indicate statistically significant differences among means relative to WT samples (*t* test: $^{**}P < 0.01$, $^{***}P < 0.001$).

production in seeds. By contrast, inhibitor treatment had no effect on the germination rate of *psy2-1* seeds (Fig. 8B). These results suggest that only PSY2 contributes to ABA synthesis for seed dormancy. They also support the conclusion that seed dormancy is independent of the ABA present in the fruit pericarp or in developing seeds but it is regulated by ABA produced in mature seeds from PSY2-derived carotenoids.

To investigate whether PSY1 and PSY2 also showed a differential contribution to ABA synthesis in other tomato tissues, we analyzed the effect of salt stress on the ABA contents of leaves and roots (Fig. 7B). The growth solution of tomato WT, *psy1-2*, and *psy2-1* seedlings cultivated hydroponically for 2 wk was changed to either salt-supplemented or unmodified (mock) media, and 24 h later, leaves and roots were separately collected. No statistical differences in ABA levels were found between WT and PSY-defective mutants in mock-treated leaf and root samples (Fig. 7B). Salt treatment increased ABA production to similar levels in leaves of the 3 genotypes. In the case of roots, however, salt stress resulted in higher ABA levels in WT and *psy1-2* but not in *psy2-1* samples (Fig. 7B). These results suggest that only PSY2 is involved in root ABA production in response to salt stress, hence confirming the specialization of PSY isoforms for ABA biosynthesis in different tissues of the tomato plant.

Discussion

PSY catalyzes the first committed and main rate-determining step of the carotenoid pathway. In most plants, several PSY isoforms control the production of carotenoids in different tissues and in response to developmental or environmental cues that require an enhanced production of these photoprotective pigments (Zhou et al. 2022). The presence of 3 PSY isoforms in tomato has been known for a long time, but genetic evidence on their physiological roles was only available for PSY1. Removal of PSY1 activity in mutants or silenced lines leads to strongly reduced levels of carotenoid pigments in ripe fruit and, to a lower extent, in corollas, but virtually unchanged carotenoid levels in green tissues, which led to conclude that PSY1 is mainly involved in carotenoid biosynthesis in chromoplasts (Bird et al. 1991; Bramley et al. 1992; D'Ambrosio et al. 2018; Fantini et al. 2013; Fraser et al. 1999; Giorio et al. 2008; Kang et al. 2014). Compared to

PSY1, *PSY2* expression is higher in leaves and increases more strongly during seedling deetiolation, supporting the conclusion that PSY2 might be the main isoform producing phytoene for carotenoids involved in photosynthesis and photoprotection (Barja et al. 2021; Bartley and Scolnik 1993; Fraser et al. 1999; Gupta et al. 2022) (Supplemental Fig. S6). *PSY3* expression levels are very low in all the tissues compared to *PSY1* and *PSY2* (Giorio et al. 2008; Stauder et al. 2018) (Supplemental Fig. S6). Similar to most members of the dicot PSY3 clade, tomato *PSY3* expression is highest in roots, where it is induced during arbuscular mycorrhizal (AM) fungi colonization (Barja et al. 2021; Stauder et al. 2018; Walter et al. 2015). Other lines of evidence concluded that the main role of PSY3 is in roots, supplying phytoene to produce carotenoids and derived SLs and apocarotenoid molecules essential for the establishment of the AM symbiosis (Baslam et al. 2013; Ezquerro et al. 2023; Fester et al. 2002; Ruiz-Lozano et al. 2016; Stauder et al. 2018). This work aimed to genetically test the hypothesis that besides the main role of PSY1 for carotenoid production in flowers and fruit (chromoplasts), PSY2 in green tissues (chloroplasts), and PSY3 in roots (leucoplasts), tomato PSY isoforms might also provide extra phytoene when a sudden requirement of carotenoid production could not be met by the isoform normally operating in a particular tissue. The generation of lines defective in PSY1 and/or PSY2 reported here provided strong genetic support to correctly frame this conclusion and it went a step beyond by unveiling a role for particular PSY isoforms in tissue-specific ABA production.

Complete loss of PSY activity in Arabidopsis results in albino seedlings (Pokhilko et al. 2015). In *Nicotiana benthamiana* (a closer relative to tomato), several genes encode PSY1, PSY2, and PSY3 homologs, but the virus-induced silencing of only those for PSY1 and PSY2 results in leaf bleaching, lower carotenoid levels, and reduced photosynthetic parameters such as ΦPSII, F_v/F_m, and NPQ (Wang et al. 2021). Consistently, we observed a seedling lethal albino phenotype in tomato lines lacking PSY1 and PSY2 but retaining a functional *PSY3* gene (Fig. 1C). This result demonstrates that PSY3 is unable to produce enough phytoene to support photosynthetic shoot development when PSY1 and PSY2 activities are missing. Indirectly, the result also provides genetic evidence supporting a root-restricted role for tomato PSY3. In the shoot, both PSY1 and PSY2 appear to provide precursors for carotenoid biosynthesis in chloroplasts under normal growth conditions (Fig. 2). However, the lower upregulation of *PSY1* expression compared to *PSY2* in response to HL (Fig. 3A) together with the reduced impact of the loss of PSY1 function on carotenoid levels and photosynthetic performance (Figs. 2 and 3) supports the model of a predominant role for PSY2 and a secondary contribution of PSY1 to carotenoid biosynthesis in tomato chloroplasts for photoprotection.

Besides chloroplasts, tomato plants accumulate very high levels of carotenoids in the chromoplasts that develop in flower corollas and ripening fruit pericarp. Loss of PSY1 had a much stronger impact than removing PSY2 on total carotenoid levels of both tissues. However, the effect in flowers (Fig. 4) was much less dramatic than in fruit (Fig. 5). Despite *PSY2* is highly expressed in petals (Giorio et al. 2008) (Supplemental Fig. S6) and PSY2 catalytic activity appears to be higher than that of PSY1 (Cao et al. 2019), complete absence of PSY2 had no effect of petal carotenoids (Fig. 4). By contrast, a 50% decrease compared to the WT was observed in PSY1-defective corollas (Fig. 4), suggesting that PSY2 only produces phytoene for carotenoid synthesis in flower chromoplasts when PSY1 activity is missing. A similar conclusion was deduced for PSY2 during fruit ripening (Gupta et al. 2022; Karniel et al. 2022). In fruit pericarp tissues, carotenoid levels were unaffected in mutants defective in PSY1 and PSY2 until the onset of ripening (Fig. 5). As chloroplasts differentiate into chromoplasts, however, the contribution of PSY1 to the production of pericarp carotenoids becomes much more predominant, mainly supported by a dramatic upregulation of gene expression (Cao et al. 2019; Giorio et al. 2008) (Supplemental Figs. S4 and S6). Without PSY1, ripe fruit accumulates a very small amount of carotenoid pigments (Fig. 5C). These carotenoids (mainly lutein and β-carotene) might be remnants of the carotenoids present in MG fruits. However, PSY activity has been measured in chromoplasts of PSY1-defective fruit (Fraser et al. 1999), and a PSY2-dependent increase in carotenoid synthesis was observed during ripening of PSY1-lacking fruit treated with different inhibitors (Gupta et al. 2022; Karniel et al. 2022). A role for PSY2 in the production of β-carotene in pericarp chromoplasts during ripening can also be deduced from the reduced accumulation of this carotenoid in *psy1 PSY2*(+/-) compared to *psy1-2* fruit (Fig. 5C). A similar role distribution has been recently described in pepper (*Capsicum annuum*), where PSY1 is the isoform supporting the bulk of pericarp carotenoid biosynthesis during fruit ripening and PSY2 is mainly associated to chloroplast-containing tissues (leaves and stems) but it also contributes to produce carotenoids in fruit chromoplasts (Jang et al. 2020; Wei et al. 2021). It has been proposed that recruitment of primary (i.e. photosynthetic) carotenoids as secondary metabolites for flower and fruit pigmentation likely required duplication and further subfunctionalization of genes encoding rate-controlling steps, including PSY (Galpaz et al. 2006; Giorio et al. 2008). In tomato, the duplicated pathway might have been originally employed for flower pigmentation and later for fruit pigmentation, explaining why all tomato species have yellow flowers but only some develop fruit chromoplasts (Galpaz et al. 2006; Giorio et al. 2008).

Besides providing strong genetic evidence supporting longstanding models on the subfunctionalization of tomato PSY1 and PSY2 isoforms to feed the carotenoid pathway, our results have unveiled isoform-specific roles in ABA production in particular tissues. In roots, salt treatment triggers an increased production of ABA in WT and *psy1* lines but not in *psy2* mutants (Fig. 7B). Besides showing that stress-induced ABA biosynthesis in tomato roots relies on PSY2 but not PSY1, the results suggest that root-localized

PSY3 does not substantially contribute to this process. This is in agreement with the conclusion that only monocot-type PSY3 enzymes (that are phylogenetically close to PSY1 and PSY2 isoforms) participate in root ABA synthesis, whereas the unrelated dicot-type PSY3 enzymes (including the tomato PSY3 isoform) are involved in root SL production (Li et al. 2008; Welsch et al. 2008; Stauder et al. 2018; Ezquerro et al. 2023). Our results also show that loss of PSY1 or PSY2 in fruit tissues differentially impacts ABA-regulated processes in the pericarp and the seeds. Genetic and pharmacological interference with carotenoid biosynthesis was previously shown to impact ABA-regulated characters such as fruit size, the onset of fruit ripening, fruit softening, and seed dormancy (Diretto et al. 2020; Galpaz et al. 2008; McQuinn et al. 2020; Zhang et al. 2009). Also, pharmacological approaches had provided evidence suggesting (but not demonstrating) that PSY2 might be involved in the production of ABA in tomato fruits (Gupta et al. 2022), most particularly in seeds (Rodriguez-Concepcion et al. 2001). Here, we showed that in the absence of PSY1, PSY2-derived carotenoids sustain the production of about two-thirds of the ABA measured in the pericarp of tomato B fruit (Fig. 7). The one-third reduction triggered phenotypes associated to low ABA levels in *psy1* fruit, including reduced fruit weight and volume, but it was not sufficient to cause changes in ethylene production or fruit hardness (Fig. 6). These results support the conclusion that different ABA thresholds are required to regulate the various processes associated with normal fruit growth and ripening. Alternatively, PSY1-derived carotenoids might be differentially used for the production of ABA in specific developmental stages or/and pericarp tissues or cell compartments, eventually causing the observed phenotypes. A differential channeling of phytoene produced by either PSY1 or PSY2 to produce carotenoids for specific ABA pools is supported by the seed germination experiments. When PSY2 is not present, PSY1 still produces about two-thirds of the ABA measured in developing and mature seeds (Fig. 7) but this relatively high amount of remaining ABA is not enough to prevent a germination delay phenotype in the *psy2* mutant (Fig. 6D). Furthermore, complete block of carotenoid (and hence downstream ABA) production in MG fruit with inhibitors did not exacerbate the seed dormancy phenotype of the *psy2* mutant (Fig. 8B). These results strongly suggest that only PSY2-derived carotenoids produced after the MG stage are used to generate the ABA that regulates dormancy in tomato seeds. Following an initial phase of tissue differentiation, tomato seed development proceeds as fruit expand with a second phase that includes the accumulation of nutrient reserves and the acquisition of germination and desiccation tolerance (De Castro and Hilhorst 2006) (Supplemental Fig. S8). When fruits reach their final size at the MG stage, seeds achieve full germinability. Later, as fruit starts to ripen, ABA production peaks and mature seeds dry and acquire their dormancy (De Castro and Hilhorst 2006). This transient accumulation of ABA is mainly supplied by the embryo (Berry and Bewley 1992). Our results confirm that ABA produced by PSY2 in seeds during ripening regulates seed dormancy (Fig. 8). Strikingly, the contribution of PSY2 to produce this ABA could not be predicted based on available expression data. Thus, *PSY2* expression is higher in developing seeds but then it drops from the MG stage in embryonic and other tissues of mature seeds (Supplemental Fig. S8). While a *PSY2*-like profile is observed for the *NOT/NCED* gene (Solyc07g056570), which encodes the first enzyme specific for ABA biosynthesis (Supplemental Fig. S8), downstream genes of the pathway such as *SIT/AAO3* (Solyc01g009230) and *FLC/ABA3* (Solyc07g066480) are more highly expressed in mature seeds (including embryos) (Supplemental Fig. S8). Although *PSY1* expression is also higher in mature seeds, little to no expression was found in embryos. These results clearly illustrate the challenges of deducing function based only on gene expression profiles.

A question arising from our data is how interference with PSY activity is specifically translated into changes in the production of ABA (Fig. 1A; Supplemental Fig. S8). A possible scenario would be the existence of metabolons channeling GGPP to ABA in cells from the root, the pericarp, or the seed. In the fruit, GGPP required to produce pericarp carotenoids and ABA during fruit ripening is mainly supplied by the GGPPS isoform SlG3 with a supporting contribution of SlG2 (Barja et al. 2021). While SlG2 can interact with both PSY1 and PSY2, no interaction was reported for SlG3 in transient coexpression assays in *N. benthamiana* leaves (Barja et al. 2021; Ezquerro et al. 2023). It is possible that interaction of SlG3 with particular PSY isoforms requires specific partners only found in tomato pericarp (to interact with PSY1) or seed (to interact with PSY2) tissues. The existence of metabolons or any other kind of metabolic channeling might explain the PSY2-specific contribution to root ABA synthesis in response to salt stress (Fig. 7B) but also why HL-triggered changes in carotenoid contents and related photosynthetic parameters are similar in *psy1* compared to *psy1 PSY2*(+/-) or in *psy2* compared to *psy2 PSY1*(+/-) seedlings (Fig. 3). If PSY channels the carotenoid pathway differently than PSY2 when there is a peak demand (e.g. after HL exposure), then reduced levels of one isoform would be expected to have little effect on total carotenoid levels. Also consistent with an isoform-specific channeling of the carotenoid pathway under some particular circumstances, the extremely low PSY2 activity present in the pericarp of *psy1* fruit appears to be more directly involved in the production of the β-carotene instead of lutein (Fig. 5C), i.e. it might be preferentially acting to produce carotenoids that could then be used as precursors for ABA synthesis (Fig. 1A). However, the channeling of specific pools of carotenoids all the way to ABA is harder to fit in a metabolon-dependent model due to the large number of reactions and the diversity of subcellular localizations reported for the enzymes involved, which include several cytosolic steps following the cleavage of β-carotene–derived xanthophyll precursors (Nambara and Marion-Poll 2005) (Fig. 1A; Supplemental Fig. S8). Alternatively, expression of specific

isoforms in particular tissue microdomains controlling root responses to salt stress, fruit ripening (directly or indirectly through ethylene), pericarp growth, or seed dormancy might explain the observed phenotypes.

In summary, we show that both PSY1 and PSY2 support carotenoid production in tomato shoots with diverging contributions in different tissues: PSY2 > PSY1 in leaves (i.e. chloroplasts), PSY1 > PSY2 in corollas, and PSY1 >> PSY2 in fruit pericarp tissues. Furthermore, we demonstrate a differential contribution to the production of ABA of PSY1 in the pericarp (to regulate fruit growth and ripening) and PSY2 in the seeds (to control dormancy) and the roots (to respond to salt stress). Further work should determine the mechanism by which the production of phytoene by given PSY isoforms is eventually channeled to produce carotenoids and ABA in particular locations for specific functions.

Materials and methods

Plant material, treatments, and sample collection

Tomato (*S. lycopersicum* var. MicroTom) plants were used for all the experiments. Seeds were surface-sterilized by a 30-min water wash followed by a 15-min incubation in 10 mL of 40% (*v*/*v*) bleach with 10 μL of Tween-20. After 3 consecutive 10-min washes with sterile Milli-Q water, seeds were germinated on plates with solid 0.5× MS medium containing 1% (*w*/*v*) agar (without vitamins or sucrose). The medium was supplemented with kanamycin (100 μg mL^{-1}) when required to select transgenic plants. Plates were incubated in a climate-controlled growth chamber (Ibercex) at 26 °C with a photoperiod of 14 h of white light (photon flux density of 50 μmol m^{-2} s^{-1}) and 10 h of darkness. After 10 to 14 d, seedlings were transferred to soil and grown under standard greenhouse conditions (14-h light at 25 ± 1 °C and 10-h dark at 22 ± 1 °C). Young leaves were collected from 4-wk-old plants and they correspond to growing leaflets from the fourth and fifth true leaves. Petal samples were collected from anthesis flowers. Fruit pericarp samples were collected at different stages, including MG (about 30 d postanthesis), B (2 to 3 d later, when the first symptoms of chlorophyll degradation and carotenoid accumulation became visually obvious), and several days after B. After collection, samples were immediately frozen in liquid nitrogen and stored at −80 °C. For fruit weight determination, 100 fully ripe individual fruits from each genotype were collected and weighted one by one using a precision scale (Kern). Fruit volume was estimated in 10 pools of 10 fruits each by measuring the displaced water volume in a graduated cylinder. Fruit hardness was quantified on harvested fruits using the 53215 Hardness Tester (Turoni) fitted with a 0.25-cm^2 plunger. Three separated points of the fruit equatorial region were used for each measurement. For inhibitor treatments, MG fruits were collected from the plant and measured to estimate their volume. Then, a Hamilton syringe was used to inject 2 to 5 μL of sterile water or inhibitor solution into the fruit. The exact volume of FSM (Sigma) or NFZ (Zorial, Syngenta) solution to inject was calculated based on the fruit volume so the final concentration in the fruits was 200 μM FSM or 50 μM NFZ. After injection, fruits were kept in a climate-controlled growth chamber at 26 °C for 12 d and then seeds were collected and immediately used for germination assays on 0.5× MS plates. Germination was scored based on root protrusion. For salt treatments, tomato WT and mutant lines were germinated and grown for 6 d on solid 0.5× MS medium and then transferred to 25-mL glass containers for hydroponic growth in half-strength Hoagland solution. The containers were covered with aluminum foil to prevent illumination of the medium (where the root developed) and placed in the climate-controlled growth chamber described above. Liquid medium was replaced every 4 d. At Day 15, the growth medium was substituted with new half-strength Hoagland solution either unsupplemented (mock) or containing 200 mM NaCl. After 24 h, samples of leaves and roots were collected separately and snap-frozen in liquid nitrogen.

Generation of CRISPR-Cas9 mutants and tomato transformation

For CRISPR-Cas9–mediated disruption of *PSY1* and *PSY2*, 1 sgRNA was designed for each gene using the online tool CRISPR-P 2.0 (Liu et al. 2017). Cloning of the CRISPR-Cas9 constructs was carried out as previously described (Barja et al. 2021) using primers listed in Supplemental Table S1. As a result, a single final binary plasmid harboring the Cas9 sequence, the *NPTII* gene providing kanamycin resistance, and the sgRNAs to disrupt *PSY1* and *PSY2* was obtained and named pDE-PSY1,2 (Supplemental Table S2). All constructs were confirmed by restriction mapping and DNA sequencing. *Agrobacterium tumefaciens* GV3101 strain was used to stably transform tomato MicroTom cotyledons with pDE-PSY1,2 as described (Barja et al. 2021). In vitro regenerated lines showing kanamycin (100 μg mL^{-1}) resistance were used for PCR amplification and sequencing of the genomic sequences. Following further segregation and PCR-based genotyping using specific primers (Supplemental Table S1), stable homozygous lines lacking the Cas9-encoding transgene were obtained and named *psy1-1*, *psy1-2*, *psy2-1*, and *psy2-2*. For the generation of double mutants lacking both PSY1 and PSY2, *psy1-2* and *psy2-1* homozygous plants were crossed and the segregating F_2 offspring was used for PCR-based genotyping of individual plants.

Photosynthetic parameters

Tomato seedlings were germinated and grown for 10 d under white light with a fluorescence photon flux density of 50 μmol m^{-2} s^{-1} (referred to as NL) and then either left under NL or transferred to a chamber with a more intense light of 300 μmol m^{-2} s^{-1} (referred to as HL) for 5 more days. Chlorophyll fluorescence measurements were carried out with a Handy FluorCam (Photon Systems Instruments). F_v/F_m was measured in seedlings incubated in the dark for 30 min to allow full relaxation of photosystems. ΦPSII was

measured at 30 PPFD with an actinic light of 3 μmol m^{-2} s^{-1}. For NPQ measurements, the following steps of actinic irradiance were used: 0, 5, 10, 20, 55, 110, 185, and 280 μmol photons m^{-2} s^{-1}.

RNA extraction and RT-qPCR analyses

Total RNA was extracted from tomato freeze-dried tissue using the PureLink RNA MINI extraction kit (Ambion). RNA was quantified using a NanoDrop 8000 spectrophotometer (Thermo Fisher Scientific) and checked for integrity by agarose gel electrophoresis. The Transcriptor First Strand cDNA Synthesis Kit (Nzytech) was used to reverse transcribe 1 μg of extracted RNA, and the generated cDNA volume (20 μL) was subsequently diluted 5-fold with Milli-Q water and stored at −20 °C for further analysis. Transcript abundance was evaluated via RT-qPCR in a reaction volume of 10 μL containing 2 μL of the cDNA dilution, 5 μL of SYBR Green Master Mix (Thermo Fisher Scientific), and 0.3 μM of each specific forward and reverse primer (Supplemental Table S1). The RT-qPCR was carried out on a QuantStudio 3 Real-Time PCR System (Thermo Fisher Scientific) using 3 independent biological samples and 3 technical replicates of each sample. Normalized transcript abundance was calculated as previously described (Simon 2003) using tomato *ACT4* (Solyc04g011500) as endogenous reference gene.

Pigment quantification

Carotenoids and chlorophylls were extracted as described (Barja et al. 2021) with some modifications. Freeze-dried materials from leaves (8 mg) were mixed with 375 μL of methanol as extraction solvent, 25 μL of a 10% (*w*/*v*) solution of canthaxanthin (Sigma) in chloroform as internal control, and glass beads. Following steps were performed as described (Barja et al. 2021). Freeze-dried flower petals and fruit pericarp tissue (20 mg) were mixed in 2-mL Eppendorf tubes with 1 mL of 2:1:1 hexane:acetone:methanol as extraction solvent, 25 μL of the canthaxanthin solution, and glass beads. After vortexing the samples, 100 μL of Milli-Q water was added to the mix. Then, samples were shaken for 1 min in a TissueLyser II (Qiagen) and then centrifuged at 4 °C for 5 min at maximum speed in a tabletop microfuge. The organic phase was transferred to a 1.5-mL tube and the rest was reextracted with 1 mL of 2:1:1 hexane:acetone:methanol. The organic phases from the 2 rounds of extraction were mixed in the same tube and evaporated using a SpeedVac. Extracted pigments were resuspended in 200 μL of acetone by using an ultrasound bath and filtered with 0.2-μm filters into amber-colored 2-mL glass vials. Separation and quantification of individual carotenoids and chlorophylls were performed as described (Barja et al. 2021). Fruit pigmentation (average red color) was measured in 3 different tomato fruit samples of each genotype using the default settings of the TomatoAnalyzer 4.0 software (https://vanderknaaplab.uga.edu/tomato_analyzer.html).

Determination of hormone levels

Ethylene production was quantified in real time with a laser-based ETD-300 ethylene detector (Sensor Sense) coupled to a VC-6 gas valve control box (Sensor Sense) that allowed simultaneous measurement of up to 5 samples. Measurements were performed for 10 min every 2 h using the continuous flow mode in 100-mL glass cuvettes containing whole tomato fruits. One empty cuvette was used as a reference. For ABA extraction, 100 mg of frozen tissue or seeds was ground with a mortar and pestle and resuspended in a solution of 80% (*v*/*v*) methanol and 1% (*v*/*v*) acetic acid with deuterium-labeled ABA as internal standard. After shaking for 1 h at 4 °C, the extract was centrifuged at maximum speed in a table top microfuge and the supernatant was collected and dried in a SpeedVac. The dry residue was dissolved in 1% (*v*/*v*) acetic acid and run through a reverse phase column (Oasis HLB) as described (Seo et al. 2011). The eluate was dissolved in 5% (*v*/*v*) acetonitrile and 1% (*v*/*v*) acetic acid and used for UHPLC chromatography with a reverse phase 2.6 μg Accucore RP-MS column of 100 mm length × 2.1 mm i.d. (Thermo Fisher Scientific). The mobile phase was 5% to 50% (*v*/*v*) acetonitrile gradient containing 0.05% (*v*/*v*) acetic acid at 400 μL min^{-1} over 21 min. Quantification of ABA was performed with a Q-Exactive mass spectrometer equipped with an Orbitrap detector (Thermo Fisher Scientific) by targeted Selected Ion 100 Monitoring (SIM). The concentrations of ABA in the extracts were determined using embedded calibration curves and the TraceFinder 4.1 SP1 software.

Statistical analyses

One-way ANOVA followed by Tukey's multiple comparisons test and Student's *t* test analyses were used to determine statistically significant differences.

Accession numbers

Sequence data from this article can be found under the following accession numbers: At5g17230 (Arabidopsis PSY), Solyc03g031860 (PSY1), Solyc02g081330 (PSY2), Solyc01g005940 (PSY3), Solyc09g089580 (E8), Solyc01g095080 (ACS2), Solyc07g056570 (NOT/NCED), Solyc01g009230 (SIT/AAO3), Solyc07g066480 (FLC/ABA3), and Solyc04g011500 (ACT4).

Acknowledgments

We thank Mª Rosa Rodriguez-Goberna and Jose Perez Beser for technical help with HPLC analyses and Tsuyoshi Nakagawa (Shimane University, Japan) for the Gateway vectors. We also thank the IBMCP Metabolomics Platform (UPV-CSIC) for hormone determinations and the members of our laboratory for helpful discussions.

Author contributions

M.E. and M.R.-C. designed the research; M.E. and E.B.-E. conducted the experiments; M.E., E.B.-E., and M.R.-C. analyzed and discussed the data; M.E. and M.R.-C. wrote the paper.

Supplemental data

The following materials are available in the online version of this article.

Supplemental Figure S1. DNA sequence alignment of *PSY1* sequences from WT and CRISPR mutants.

Supplemental Figure S2. DNA sequence alignment of *PSY2* sequences from WT and CRISPR mutants.

Supplemental Figure S3. Protein sequence alignment of PSY1 and PSY2 sequences from WT and CRISPR mutants.

Supplemental Figure S4. Representative phenotypes of tomato mutants defective in PSY1 or PSY2.

Supplemental Figure S5. PCR genotyping of mutant alleles.

Supplemental Figure S6. *PSY1*, *PSY2*, and *PSY3* transcript levels in different tissues.

Supplemental Figure S7. Expression profile of *PSY1* and *PSY2* in the fruit pericarp during development.

Supplemental Figure S8. Expression profile of ABA biosynthetic genes in developing seeds.

Supplemental Table S1. Primers used in this work.

Supplemental Table S2. CRISPR-Cas9 constructs and cloning details.

Funding

This work was funded by grants from Spanish Agencia Estatal de Investigación MCIN/AEI /10.13039/501100011033 and European Commission NextGeneration EU/PRTR and PRIMA programs to M.R.-C. (PID2020-115810GB-I00 and UToPIQ-PCI2021-121941). M.R.-C. is also supported by Consejo Superior de Investigaciones Cientificas (202040E299) and Generalitat Valenciana (PROMETEU/2021/056 and AGROALNEXT/2022/067). M.E. and E.B.-E. received predoctoral fellowships from MCIN/AEI (BES-2017-080652) and Colombia's Colciencias Doctorado Exterior program (MINCIENCIAS885/2020), respectively.

Conflict of interest statement. None declared.

References

Ariizumi T, Kishimoto S, Kakami R, Maoka T, Hirakawa H, Suzuki Y, Ozeki Y, Shirasawa K, Bernillon S, Okabe Y, et al. Identification of the carotenoid modifying gene PALE YELLOW PETAL 1 as an essential factor in xanthophyll esterification and yellow flower pigmentation in tomato (*Solanum lycopersicum*). Plant J. 2014:**79**(3):453–465. https://doi.org/10.1111/tpj.12570

Barja MV, Ezquerro M, Beretta S, Diretto G, Florez-Sarasa I, Feixes E, Fiore A, Karlova R, Fernie AR, Beekwilder J, et al. Several geranylgeranyl diphosphate synthase isoforms supply metabolic substrates for carotenoid biosynthesis in tomato. New Phytol. 2021:**231**(1):255–272. https://doi.org/10.1111/nph.17283

Bartley GE, Scolnik PA. cDNA cloning, expression during development, and genome mapping of PSY2, a second tomato gene encoding phytoene synthase. J Biol Chem. 1993:**268**(34):25718–25721. https://doi.org/10.1016/S0021-9258(19)74448-2

Baslam M, Esteban R, García-Plazaola JI, Goicoechea N. Effectiveness of arbuscular mycorrhizal fungi (AMF) for inducing the accumulation of major carotenoids, chlorophylls and tocopherol in green and red leaf lettuces. App Microbiol Biotechnol. 2013:**97**(7):3119–3128. https://doi.org/10.1007/s00253-012-4526-x

Berry T, Bewley JD. A role for the surrounding fruit tissues in preventing the germination of tomato (*Lycopersicon esculentum*) seeds: a consideration of the osmotic environment and abscisic acid. Plant Physiol. 1992:**100**(2):951–957. https://doi.org/10.1104/pp.100.2.951

Bird CR, Ray JA, Fletcher JD, Boniwell JM, Bird AS, Teulieres C, Blain I, Bramley P, Schuch W. Using antisense RNA to study gene function: inhibition of carotenoid biosynthesis in transgenic tomatoes. Nat Biotechnol. 1991:**9**(7):635–639. https://doi.org/10.1038/nbt0791-635

Bramley P, Teulieres C, Blain I, Bird C, Schuch W, Holloway R. Biochemical characterization of transgenic tomato plants in which carotenoid synthesis has been inhibited through the expression of antisense RNA to pTOM5. Plant J. 1992:**2**(3):343–349. https://doi.org/10.1111/j.1365-313X.1992.00343.x

Cao H, Luo H, Yuan H, Eissa MA, Thannhauser TW, Welsch R, Hao YJ, Cheng L, Li L. A neighboring aromatic-aromatic amino acid combination governs activity divergence between tomato phytoene synthases. Plant Physiol. 2019:**180**(4):1988–2003. https://doi.org/10.1104/pp.19.00384

D'Ambrosio C, Stigliani AL, Giorio G. CRISPR/Cas9 editing of carotenoid genes in tomato. Transg Res. 2018:**27**(4):367–378. https://doi.org/10.1007/s11248-018-0079-9

De Castro RD, Hilhorst HWM. Hormonal control of seed development in GA- and ABA-deficient tomato (*Lycopersicon esculentum* Mill. cv. Moneymaker) mutants. Plant Sci. 2006:**170**(3):462–470. https://doi.org/10.1016/j.plantsci.2005.09.014

Diretto G, Frusciante S, Fabbri C, Schauer N, Busta L, Wang Z, Matas AJ, Fiore A, Rose J KC, Fernie AR, et al. Manipulation of β-carotene levels in tomato fruits results in increased ABA content and extended shelf life. Plant Biotechnol J. 2020:**18**(5):1185–1199. https://doi.org/10.1111/pbi.13283

Ezquerro E, Li C, Pérez-Pérez J, Burbano-Erazo E, Barja MV, Wang Y, Dong L, Lisón P, López-Gresa M-P, Bouwmeester HJ, et al. Tomato geranylgeranyl diphosphate synthase isoform 1 is involved in the stress-triggered production of diterpenes in leaves and strigolactones in roots. New Phytol. https://doi.org/10.1111/nph.19109, 28 June 2023, preprint: not peer reviewed.

Fantini E, Falcone G, Frusciante S, Giliberto L, Giuliano G. Dissection of tomato lycopene biosynthesis through virus-induced gene silencing. Plant Physiol. 2013:**163**(2):986–998. https://doi.org/10.1104/pp.113.224733

Fester T, Schmidt D, Lohse S, Walter MH, Giuliano G, Bramley PM, Fraser PD, Hause B, Strack D. Stimulation of carotenoid metabolism in arbuscular mycorrhizal roots. Planta 2002:**216**(1):148–154. https://doi.org/10.1007/s00425-002-0917-z

Fraser PD, Kiano JW, Truesdale MR, Schuch W, Bramley PM. Phytoene synthase-2 enzyme activity in tomato does not contribute to carotenoid synthesis in ripening fruit. Plant Mol Biol. 1999:**40**(4):687–698. https://doi.org/10.1023/A:1006256302570

Fray RG, Grierson D. Identification and genetic analysis of normal and mutant phytoene synthase genes of tomato by sequencing, complementation and co-suppression. Plant Mol Biol. 1993:**22**(4):589–602. https://doi.org/10.1007/BF00047400

Galpaz N, Ronen G, Khalfa Z, Zamir D, Hirschberg J. A chromoplast-specific carotenoid biosynthesis pathway is revealed by cloning of the tomato white-flower locus. Plant Cell 2006:**18**(8):1947–1960. https://doi.org/10.1105/tpc.105.039966

Galpaz N, Wang Q, Menda N, Zamir D, Hirschberg J. Abscisic acid deficiency in the tomato mutant high-pigment 3 leading to increased plastid number and higher fruit lycopene content. Plant J. 2008:**53**(5):717–730. https://doi.org/10.1111/j.1365-313X.2007.03362.x

Giorio G, Stigliani AL, D'Ambrosio C. Phytoene synthase genes in tomato (*Solanum lycopersicum* L.)—new data on the structures, the deduced amino acid sequences and the expression patterns. FEBS J. 2008:**275**(3):527–535. https://doi.org/10.1111/j.1742-4658.2007.06219.x

Groot SPC, Karssen CM. Dormancy and germination of abscisic acid-deficient tomato seeds' studies with the sitiens mutant. Plant Physiol. 1992:**99**(3):952–958. https://doi.org/10.1104/pp.99.3.952

Gupta P, Rodriguez-Franco M, Bodanapu R, Sreelakshmi Y, Sharma R. Phytoene synthase 2 in tomato fruits remains functional and contributes to abscisic acid formation. Plant Sci. 2022:**316**:111177. https://doi.org/10.1016/j.plantsci.2022.111177

Hirschberg J. Carotenoid biosynthesis in flowering plants. Curr Opin Plant Biol. 2001:**4**(3):210–218. https://doi.org/10.1016/S1369-5266(00)00163-1

Jang SJ, Jeong HB, Jung A, Kang MY, Kim S, Ha SH, Kwon JK, Kang BC. Phytoene synthase 2 can compensate for the absence of PSY1 in the control of color in *Capsicum* fruit. J Exp Bot. 2020:**71**(12):3417–3427. https://doi.org/10.1093/jxb/eraa155

Kachanovsky DE, Filler S, Isaacson T, Hirschberg J. Epistasis in tomato color mutations involves regulation of phytoene synthase 1 expression by cis-carotenoids. Proc Natl Acad Sci USA. 2012:**109**(46):19021–19026. https://doi.org/10.1073/pnas.1214808109

Kang B, Gu Q, Tian P, Xiao L, Cao H, Yang W. A chimeric transcript containing Psy1 and a potential mRNA is associated with yellow flesh color in tomato accession PI 114490. Planta 2014:**240**(5):1011–1021. https://doi.org/10.1007/s00425-014-2052-z

Karniel U, Adler Berke N, Mann V, Hirschberg J. Perturbations in the carotenoid biosynthesis pathway in tomato fruit reactivate the leaf-specific phytoene synthase 2. Front Plant Sci. 2022:**13**:844748. https://doi.org/10.3389/fpls.2022.844748

Leng P, Yuan B, Guo Y, Chen P. The role of abscisic acid in fruit ripening and responses to abiotic stress. J Exp Bot. 2014:**65**(16):4577–4588. https://doi.org/10.1093/jxb/eru204

Li F, Vallabhaneni R, Wurtzel ET. PSY3, a new member of the phytoene synthase gene family conserved in the Poaceae and regulator of abiotic stress-induced root carotenogenesis. Plant Physiol. 2008:**146**(3):1333–1345. https://doi.org/10.1104/pp.107.111120

Liu H, Ding Y, Zhou Y, Jin W, Xie K, Chen LL. CRISPR-P 2.0: an improved CRISPR-Cas9 tool for genome editing in plants. Mol Plant. 2017:**10**(3):530–532. https://doi.org/10.1016/j.molp.2017.01.003

McQuinn RP, Gapper NE, Gray AG, Zhong S, Tohge T, Fei Z, Fernie AR, Giovannoni JJ. Manipulation of ZDS in tomato exposes carotenoid- and ABA-specific effects on fruit development and ripening. Plant Biotechnol J. 2020:**18**(11):2210–2224. https://doi.org/10.1111/pbi.13377

Moreno JC, Mi J, Alagoz Y, Al-Babili S. Plant apocarotenoids: from retrograde signaling to interspecific communication. Plant J. 2021:**105**(2):351–375. https://doi.org/10.1111/tpj.15102

Nambara E, Marion-Poll A. Abscisic acid biosynthesis and catabolism. Annu Rev Plant Biol. 2005:**56**(1):165–185. https://doi.org/10.1146/annurev.arplant.56.032604.144046

Nitsch L, Kohlen W, Oplaat C, Charnikhova T, Cristescu S, Michieli P, Wolters-Arts M, Bouwmeester H, Mariani C, Vriezen WH, et al. ABA-deficiency results in reduced plant and fruit size in tomato. J Plant Physiol. 2012:**169**(9):878–883. https://doi.org/10.1016/j.jplph.2012.02.004

Pokhilko A, Bou-Torrent J, Pulido P, Rodríguez-Concepción M, Ebenhöh O. Mathematical modelling of the diurnal regulation of the MEP pathway in *Arabidopsis*. New Phytol. 2015:**206**(3):1075–1085. https://doi.org/10.1111/nph.13258

Rodríguez-Concepción M, Ahumada I, Diez-Juez E, Sauret-Güeto S, Lois LM, Gallego F, Carretero-Paulet L, Campos N, Boronat A. 1-Deoxy-D-xylulose 5-phosphate reductoisomerase and plastid isoprenoid biosynthesis during tomato fruit ripening. Plant J. 2001:**27**(3):213–222. https://doi.org/10.1046/j.1365-313x.2001.01089.x

Rodríguez-Concepción M, Avalos J, Bonet ML, Boronat A, Gomez-Gomez L, Hornero-Mendez D, Limon MC, Meléndez-Martínez AJ, Olmedilla-Alonso B, Palou A, et al. A global perspective on carotenoids: metabolism, biotechnology, and benefits for nutrition and health. Progr Lipid Res. 2018:**70**:62–93. https://doi.org/10.1016/j.plipres.2018.04.004

Ruiz-Lozano JM, Aroca R, Zamarreño ÁM, Molina S, Andreo-Jiménez B, Porcel R, García-Mina JM, Ruyter-Spira C, López-Ráez JA. Arbuscular mycorrhizal symbiosis induces strigolactone biosynthesis under drought and improves drought tolerance in lettuce and tomato. Plant Cell Environ. 2016:**39**(2):441–452. https://doi.org/10.1111/pce.12631

Seo M, Jikumaru Y, Kamiya Y. Profiling of hormones and related metabolites in seed dormancy and germination studies. Meth Mol Biol. 2011:**773**:99–111. https://doi.org/10.1007/978-1-61779-231-1_7

Simon P. Q-Gene: processing quantitative real-time RT-PCR data. Bioinformatics 2003:**19**(11):1439–1440. https://doi.org/10.1093/bioinformatics/btg157

Stauder R, Welsch R, Camagna M, Kohlen W, Balcke GU, Tissier A, Walter MH. Strigolactone levels in dicot roots are determined by an ancestral symbiosis-regulated clade of the PHYTOENE SYNTHASE gene family. Front Plant Sci. 2018:**9**:255. https://doi.org/10.3389/fpls.2018.00255

Sun T, Yuan H, Cao H, Yazdani M, Tadmor Y, Li L. Carotenoid metabolism in plants: the role of plastids. Mol Plant. 2018:**11**(1):58–74. https://doi.org/10.1016/j.molp.2017.09.010

Walter MH, Stauder R, Tissier A. Evolution of root-specific carotenoid precursor pathways for apocarotenoid signal biogenesis. Plant Sci. 2015:**233**:1–10. https://doi.org/10.1016/j.plantsci.2014.12.017

Wang Z, Zhang L, Dong C, Guo J, Jin L, Wei P, Li F, Zhang X, Wang R. Characterization and functional analysis of phytoene synthase gene family in tobacco. BMC Plant Biol. 2021:**21**(1):32. https://doi.org/10.1186/s12870-020-02816-3

Wei X, Meng C, Yuan Y, Nath UK, Zhao Y, Wang Z, Yang S, Li L, Niu L, Yao Q, et al. CaPSY1 gene plays likely the key role in carotenoid metabolism of pepper (*Capsicum annuum*) at ripening. Funct Plant Biol. 2021:**48**(2):141–155. https://doi.org/10.1071/FP19287

Welsch R, Wüst F, Bär C, Al-Babili S, Beyer P. A third phytoene synthase is devoted to abiotic stress-induced abscisic acid formation in rice and defines functional diversification of phytoene synthase genes. Plant Physiol. 2008:**147**(1):367–380. https://doi.org/10.1104/pp.108.117028

Zhang M, Yuan B, Leng P. The role of ABA in triggering ethylene biosynthesis and ripening of tomato fruit. J Exp Bot. 2009:**60**(6):1579–1588. https://doi.org/10.1093/jxb/erp026

Zhou X, Rao S, Wrightstone E, Sun T, Lui ACW, Welsch R, Li L. Phytoene synthase: the key rate-limiting enzyme of carotenoid biosynthesis in plants. Front Plant Sci. 2022:**13**:884720. https://doi.org/10.3389/fpls.2022.884720